Letter
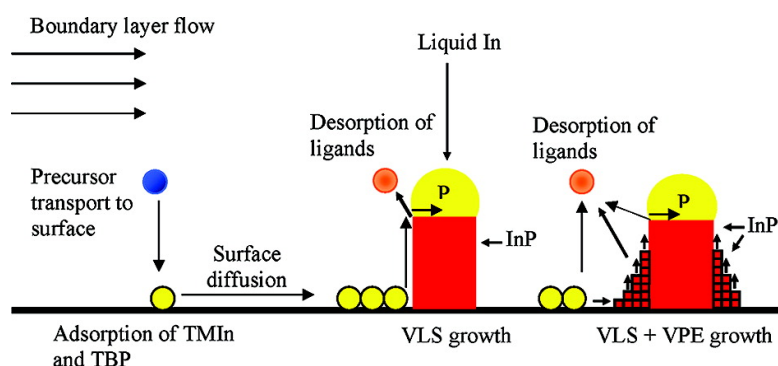
Kinetic Control of Self-Catalyzed Indium Phosphide Nanowires, Nanocones, and Nanopillars

Robyn L. Woo, Li Gao, Niti Goel, Mantu K. Hudait, Kang L. Wang, Suneel Kodambaka, and Robert F. Hicks

More About This Article

Additional resources and features associated with this article are available within the HTML version:

- Supporting Information
- Access to high resolution figures
- Links to articles and content related to this article
- Copyright permission to reproduce figures and/or text from this article

View the Full Text HTML

Kinetic Control of Self-Catalyzed Indium Phosphide Nanowires, Nanocones, and Nanopillars

Robyn L. Woo,[†] Li Gao,[†] Niti Goel,[‡] Mantu K. Hudait,[§] Kang L. Wang,[||]
Suneel Kodambaka,[⊥] and Robert F. Hicks*,[†,⊥]

Departments of Chemical and Biomolecular Engineering, Electrical Engineering, and Materials Science and Engineering, University of California, Los Angeles, California 90095, Intel Corporation, Santa Clara, California 95052, and Intel Corporation, Hillsboro, Oregon 97124

ABSTRACT

The morphological phase diagram is reported for InP nanostructures grown on InP (111)B as a function of temperature and V/III ratio. Indium droplets were used as the catalyst and were generated in situ in the metalorganic vapor-phase epitaxy reactor. Three distinct nanostructures were observed: wires, cones, and pillars. It is proposed that the shape depends on the relative rates of indium phosphide deposition via the vapor−liquid−solid (VLS) and vapor-phase epitaxy (VPE) processes. The rate of VLS is relatively insensitive to temperature and results in vertical wire growth starting at 350 °C. By contrast, the rate of VPE accelerates with temperature and drives the lateral growth of cones at 385 °C and then pillars at 400 °C.

Semiconductor nanowires show great potential for applications in electronics and photonics.[1−9] Most nanowires are prepared by the vapor−liquid−solid process utilizing a metal catalyst, such as gold.[10] The liquid alloy droplet captures the precursor materials and catalyzes crystal growth at the liquid−solid interface. Nanowires with nontapered and/or tapered morphologies are obtained depending on the conditions,[11−17] and these different shapes significantly affect their electrical, optical, and mechanical properties.[18−22] Recently, in situ electron microscopy studies have provided fundamental insight into the nanowire nucleation and growth process.[23−27]

For III−V materials, different methods have been used to synthesize the nanostructures, including metalorganic vapor-phase epitaxy (MOVPE), molecular beam epitaxy (MBE), and chemical beam epitaxy (CBE).[28−30] Nanowires have been grown without the aid of catalysts, for example, using patterned oxide templates, and excellent control over the wire size and shape has been achieved.[14,31,32] The kinetics and mechanism of III−V nanowire growth using Au catalysis has been investigated and is relatively well understood.[33−36]

On the other hand, little is known about III−V nanowire growth whereby group III metal droplets are used to self-catalyze deposition.[37−41]

The aim of this work is to investigate the effect of substrate temperature and V/III mole ratio on the self-catalyzed deposition of indium phosphide nanowires using liquid indium droplets. Scanning electron microscopy reveals that the shapes of the indium phosphide nanostructures can be precisely controlled in the MOVPE process to synthesize wires, cones, or pillars. We propose that the crystal morphology is determined by the relative rates of InP deposition via the vapor−liquid−solid (VLS) and vapor-phase epitaxy (VPE) mechanisms.

The experiments were carried out in a Veeco D125 MOVPE reactor using trimethylindium (TMIn) and *tert*-butylphosphine (TBP). The nanostructures were grown on InP (111)B substrates. The samples were placed in the reactor and annealed at 550 °C in 1.0 mmol/min of TBP for 5 min. Then the temperature was lowered to between 350 and 400 °C, and the indium droplets were deposited by feeding 10−50 μmol/min of TMIn for 0.2−0.5 min. Next, the InP nanostructures were deposited by feeding TBP and TMIn at P/In mole ratios between 40 and 133. A constant TBP mole fraction of 7.2×10^{-4} was maintained in the hydrogen gas flow at 60 Torr total pressure. Following 9.0 min of growth, the samples were cooled down in H_2 over 10 min to 30 °C. Note that the substrate temperature in the MOVPE reactor is known to ±25 °C.

* Corresponding author, rhicks@ucla.edu.
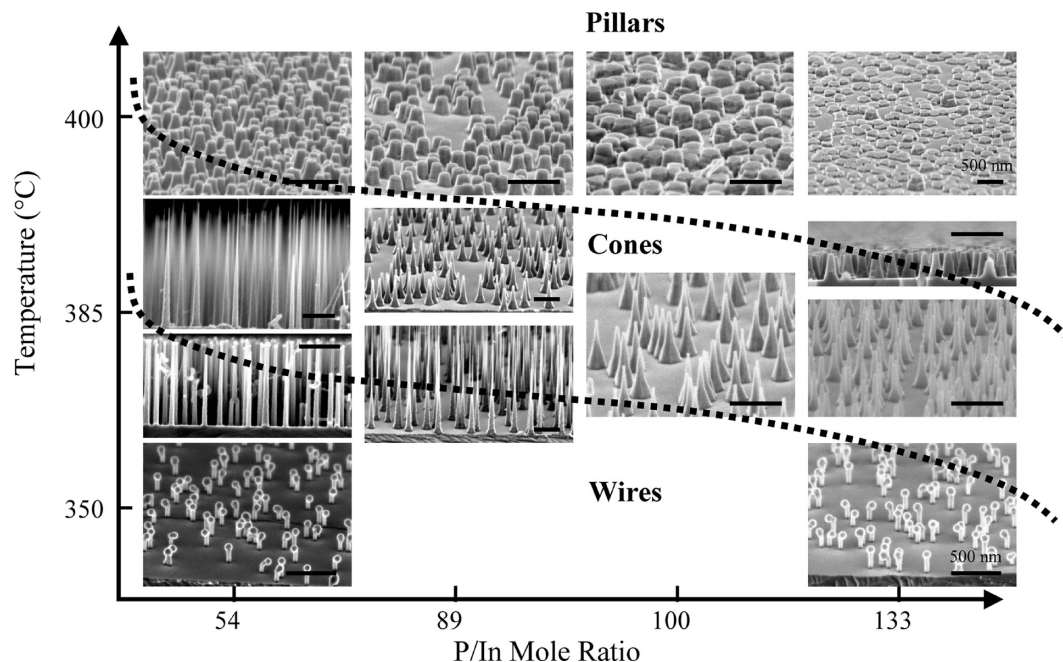† Department of Chemical and Biomolecular Engineering, University of California.
‡ Intel Corporation, Santa Clara.
§ Intel Corporation, Hillsboro.
|| Department of Electrical Engineering, University of California.
⊥ Department of Materials Science and Engineering, University of California.

Figure 1. Phase diagram of InP nanostructures as a function of temperature and P/In molar ratio.

The surfaces were imaged using a Hitachi S4700 field emission scanning electron microscope (SEM). The data were processed with the aid of ImageJ. For each experiment, at least 10 SEM images consisting of over 400 nanostructures were analyzed to obtain the average diameter, width, height, and areal density. Images of the indium droplets were obtained prior to growth as well. The droplet diameters were 30, 68, and 86 $\pm$ 8 nm, and their densities were 7.2×10^9, 3.6×10^9, and $1.5 \times 10^9 \pm 0.3 \times 10^9$ cm^{-2} for deposition at 350, 385, and 400 °C, respectively.

The InP nanostructures grown using In droplets as a function of temperature and P/In mole ratio are shown in Figure 1. Three characteristic shapes are observed as the temperature is raised from 350 to 400 °C. At 350 °C, nanowires are produced with a fixed diameter of ~50 nm regardless of their length. To highlight the morphology, the growth time is kept to 2 min at this temperature, whereas at 385 and 400 °C, the growth time is 9 min. At 385 °C, nanocones are formed which exhibit a wide hexagonal base, 100−200 nm across, and taper down to a width of 10 to 50 nm at the tip. Finally at 400 °C, nanopillars are formed. These structures are low-aspect-ratio cylinders with hexagonal bases of 230−270 nm in width.

Increasing the growth temperature at a fixed P/In mole ratio causes the formation of conical and pillar-shaped InP nanostructures rather than wires. We note that increasing the P/In mole ratio from 54 to 133 at a fixed temperature does not significantly affect the shape. The height of the nanostructures, however, decreases as the TMIn flux is reduced, as clearly seen at 400 °C. The dotted lines in Figure 1 delineate isomorphic contours. These data reveal that nanowires grow best at low temperature and low P/In mole ratio, while hexagonal pillars grow best at high temperature and high P/In mole ratio. In the following sections, we focus on the growth aspects of the nanowires and nanopillars.
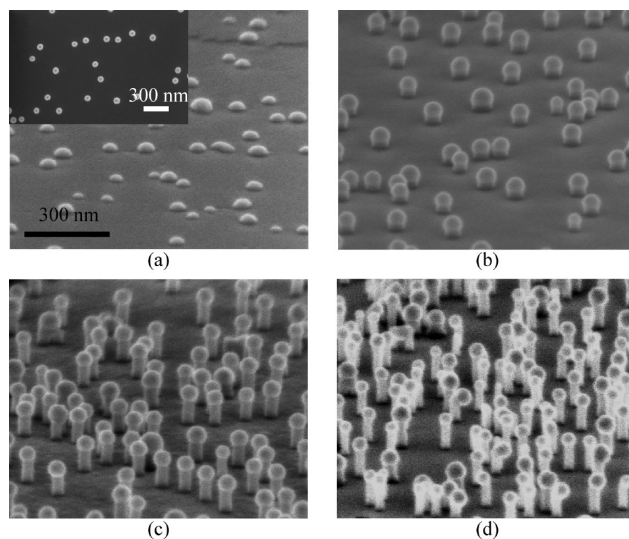
Figure 2. Images of InP nanowires grown at 350 °C, depicting (a) In catalysts, (b) InP wires after 1 min, (c) InP wires after 3 min, and (d) InP wires after 4 min of growth.

Shown in Figure 2 are a series of SEM images of nanowires acquired as a function of deposition time at 350 °C and P/In mole ratio of 100. The inset shows a top-view image of the sample. Prior to introducing the TBP, indium droplets were deposited by feeding 20 μmol/min of TMIn for 30 s (Figure 2a). Here, we see a homogeneous distribution of droplets of average size 78 $\pm$ 5 nm. Upon feeding 1.0 mmol/min TBP along with the TMIn, the nanowires begin growing with the indium catalyst at the top (confirmed by energy dispersive X-ray analysis). The wire diameters are 51 $\pm$ 5 nm or 65 $\pm$ 0.6% of the In droplet diameter. The average droplet diameter and wire width remain constant throughout the process, while the average wire length increases linearly at a rate of ~27 nm/min. (Plots of wire lengths and diameters versus deposition time are shown in
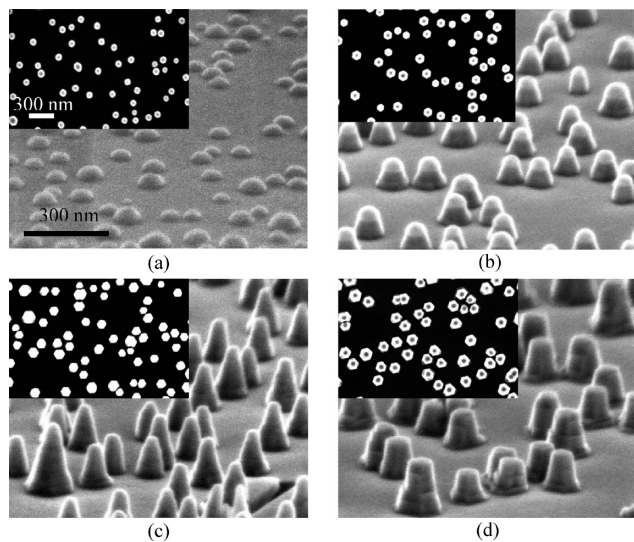
Figure 3. Images of InP nanopillars grown at 400 °C, depicting (a) In catalysts, (b) InP pillars after 1 min, (c) InP pillars after 2 min, and (d) InP pillars after 5 min of growth.

Figure 4. Schematic diagram of the MOVPE growth mechanisms for InP nanowires, nanocones, and nanopillars.

Figure S1 of the Supporting Information.) Note that the melting point of indium is 157 °C,[42] so we expect liquid droplets during growth. The observation of wires with In droplets at the wire tips is consistent with nanowire synthesis by the VLS mechanism.[10]

Shown in Figure 3 are a series of SEM images of nanopillars acquired as a function of deposition time at 400 °C and P/In mole ratio of 100. The indium droplets were initially formed by feeding 50 μmol/min of TMIn for 12 s (Figure 3a). A homogeneous distribution of droplets is observed with average size of 86 ± 8 nm. Upon introducing the TMIn and TBP, InP nanopillars with hexagonal bases grow up as shown in parts b and d of Figure 3. At the 1 min mark, the In droplets can still be discerned in the image, whereas after 2 min of growth, they are no longer evident. With continued deposition, facets form along the {110} sidewalls of the pillars (cf. Figure 3d). These results show that the pillar height increases during the first 2 min of growth to a maximum value of 150 nm and, thereafter, remains constant. On the other hand, the pillar base width continuously increases throughout the process from 85 nm to 141 ± 20 nm in 5 min (see Figure S2 of Supporting Information). Even wider bases of 250 ± 35 nm are recorded in Figure 1, top row. The above results show that vertical growth of the nanopillars occurs with consumption of the indium droplets and ceases after they are gone. It follows then that broadening of the pillar bases occurs via lateral deposition along the sidewalls from the vapor, i.e., by vapor-phase epitaxy of indium phosphide on the exposed {110} planes.[43]

The shape of the observed nanostructures can be explained by a simple model, which accounts for the two competing growth mechanisms, VLS and VPE. A schematic of the elementary processes that occur during deposition is presented in Figure 4. The metalorganic precursors transport to the InP (111)B substrate and dissociatively adsorb onto the surface. We would like to point out that the adsorption rate of III/V metalorganic precursors at 350−400 °C on InP
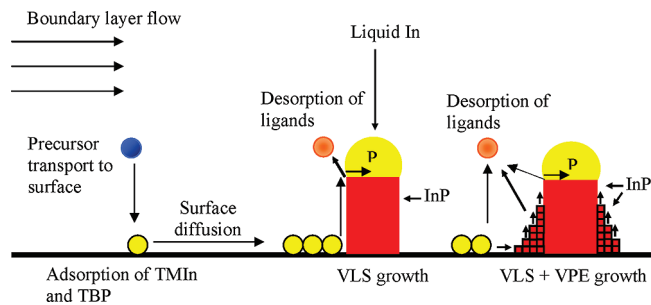
surfaces (e.g., (001)) is high due to dative bonding between the empty p orbitals on the In atoms and the filled lone pairs on the P atoms.[44] This is in contrast to the silicon and germanium system and the hydride precursors used for the growth of those nanowires.[45,46] Once adsorbed, the TMIn and TBP diffuse across the surface until they find an active site for decomposition. This process occurs by the stepwise desorption of the alkyl ligands from the In and P atoms. For VLS growth, the liquid indium catalyzes the decomposition reaction, in particular, of TBP because TBP does not decompose at 350 °C and results in dissolution of indium and phosphorus into the droplet. Evidence of dissolution of indium into the droplet is provided by the fact that the indium droplet size remains constant while the InP nanowire is growing. Incorporation of the In and P atoms from the droplet at the liquid−solid interface results in the formation of the indium phosphide nanowire.

We propose that the VLS growth rate is limited by the diffusion of the adsorbed precursors across the substrate surface for the cases, where the wire length is less than the diffusion length of adsorbed precursors. This is supported by our experiments, which show that the vertical growth rate of the nanowires is relatively independent of temperature. Furthermore, the growth rate decreases with increasing wire diameter as expected for a fixed supply of diffusing species from the substrate (see Figure S3 of the Supporting Information). These results are consistent with previous studies, which predict similar diameter-dependent wire growth kinetics when the rate-limiting step is the surface diffusion of adsorbed species to the liquid droplets.[24,47,48]

In the case of vapor-phase epitaxy, the same elementary steps are involved in deposition, except that now desorption of the alkyl ligands occurs directly from the indium phosphide surface.[43,49] The In and P atoms released on the surface diffuse to the base of the nanowire where they nucleate and grow InP crystallites laterally by the "step-flow" mode on exposed {110} planes. In contrast to VLS, the rate-limiting step for VPE is desorption of the alkyl groups from the InP surface. The rate of this reaction obeys an Arrhenius relationship with an exponential dependence on temperature.[43,49]

A schematic plot of the VLS and VPE growth rates as a function of temperature is shown in Figure 5. For VLS, the rate-limiting surface diffusion step does not strongly depend on temperature, whereas for VPE, the rate-limiting alkyl
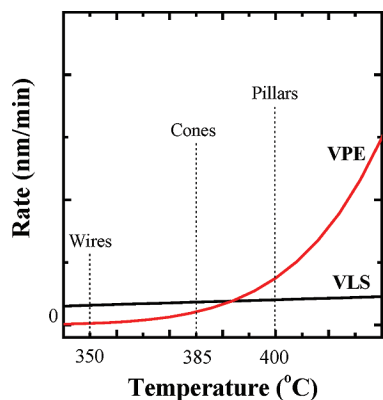
Figure 5. Schematic plot of the VLS and VPE growth rates as a function of temperature.

desorption reaction increases exponentially with temperature.[43] At 350 °C, only VLS occurs, resulting in the formation of high-aspect-ratio nanowires. At 385 °C, VPE becomes significant relative to VLS, and lateral growth at the base of the nanowires is observed. Since the rate of supply of indium to the droplets is less than the rate of loss of In from the droplets, their size shrinks slowly with time, until they finally disappear. This process yields the nanocones shown in Figure 1. At 400 °C, the rate of VPE has increased to the point where the In loss rate from the droplets is significantly higher than the supply rate to the droplets, resulting in their rapid consumption and the sustained lateral growth of low-aspect-ratio nanopillars.

The model proposed in Figure 4 can explain the different types of nanostructures reported in the literature.[11−16] When the temperature is high enough to support VPE in addition to VLS, deposition will occur at the sidewall of the wires, resulting in tapered shapes.[11,14,16] At even higher temperatures, where the rate of VPE is much greater than that of VLS, crystal growth takes place along the entire surface of the nanowire by a layer-by-layer mode,[43] and the resulting shape is no longer tapered.[15]

Another way to achieve tapered nanowires in the VLS process is via accumulation at or loss of indium from the liquid droplet during growth.[12,13] If too much TMIn is being supplied to the droplet, it will grow with time, causing the diameter of nanowires to increase slowly. Conversely, if not enough TMIn is being supplied to the droplet, it will shrink with time, causing the nanowire diameter to gradually decrease. This type of tapering can be identified by the characteristic smooth sidewall of the nanowires and lack of faceting.

In summary, for self-catalyzed growth of indium phosphide from indium droplets, nanowires, nanocones, and nanopillars are produced by increasing the temperature from 350 to 400 °C. The particular type of structure formed is governed by the relative rate of InP deposition by VLS versus VPE. An understanding of the mechanisms underlying crystal growth at the nanoscale is crucial to developing methods for large-scale fabrication of these structures with precisely controlled size and shape.

Supporting Information Available: Experimental details and growth parameters. This material is available free of charge via the Internet at http://pubs.acs.org.

References
(1) Cui, Y.; Lieber, C. M. *Science* **2001**, *291*, 851.
(2) Wang, J. F.; Gudiksen, M. S.; Duan, X. F.; Cui, Y.; Lieber, C. M. *Science* **2001**, *293*, 1455.
(3) Cui, Y.; Wei, Q. Q.; Park, H. K.; Lieber, C. M. *Science* **2001**, *293*, 1289.
(4) Duan, X. F.; Huang, Y.; Cui, Y.; Wang, J. F.; Lieber, C. M. *Nature* **2001**, *409*, 66.
(5) Björk, M. T.; Ohlsson, B. J.; Sass, T.; Persson, A. I.; Thelander, C.; Magnusson, M. H.; Deppert, K.; Wallenberg, L. R.; Samuelson, L. *Appl. Phys. Lett.* **2002**, *80*, 1058.
(6) Johnson, J. C.; Choi, H.-J.; Knutsen, K. P.; Schaller, R. D.; Yang, P.; Saykally, R. J. *Nat. Mater.* **2002**, *1*, 106.
(7) Bryllert, T.; Wernersson, L.-E.; Lowgren, T.; Samuelson, L. *Nanotechnology* **2006**, *17*, S227.
(8) Nilsson, H. A.; Thelander, C.; Froberg, L. E.; Wagner, J. B.; Samuelson, L. *Appl. Phys. Lett.* **2006**, *89*, 163101.
(9) Doh, Y.-J.; van Dam, J. A.; Roest, A. L.; Bakkers, E. P. A. M.; Kouwenhoven, L. P.; De Franceschi, S. *Science* **2005**, *309*, 272.
(10) Wagner, R. S.; Ellis, W. C. *Appl. Phys. Lett.* **1964**, *4*, 89.
(11) Haraguchi, K.; Katsuyama, T.; Hiruma, K.; Ogawa, K. *Appl. Phys. Lett.* **1992**, *60*, 745.
(12) Novotny, C. J.; Yu, P. K. L. *Appl. Phys. Lett.* **2005**, *87*, 203111.
(13) Hannon, J. B.; Kodambaka, S.; Ross, F. M.; Tromp, R. M. *Nature* **2006**, *440*, 69.
(14) Mohan, P.; Motohisa, J.; Fukui, T. *Nanotechnology* **2005**, *16*, 2903.
(15) Jin, C.-B.; Yang, J.-E.; Jo, M.-H. *Appl. Phys. Lett.* **2006**, *88*, 193105.
(16) Chen, C.; Plante, M. C.; Fradin, C.; LaPierre, R. R. *J. Mater. Res.* **2006**, *21*, 2801.
(17) Geelhaar, L. *Appl. Phys. Lett.* **2007**, *91*, 093113.
(18) Wagner, R. S. *Whisker Technology*; Wiley: New York, 1970.
(19) Wong, E. W.; Sheehan, P. E.; Lieber, C. M. *Science* **1997**, *277*, 1971.
(20) Persson, M. P.; Xu, H. Q. *Appl. Phys. Lett.* **2002**, *81*, 1309.
(21) Bao, J.; Bell, D.; Capasso, F.; Mårtensson, T.; Wagner, J. B.; Trägårdh, J.; Samuelson, L. *Nano Lett.* **2008**, *8*, 836.
(22) Chuang, L. C.; Moewe, M.; Crankshaw, S.; Chang-Hasnain, C. *Appl. Phys. Lett.* **2008**, *92*, 013121.
(23) Hannon, J. B.; Kodambaka, S.; Ross, F. M.; Tromp, R. M. *Nature* **2006**, *440*, 69.
(24) Kodambaka, S.; Tersoff, J.; Reuter, M. C.; Ross, F. M. *Phys. Rev. Lett.* **2006**, *96*, 096105.
(25) Kodambaka, S.; Tersoff, J.; Reuter, M. C.; Ross, F. M. *Science* **2007**, *316*, 729.
(26) Hofmann, S.; Sharma, R.; Wirth, C. T.; Cervantes-Sodi, F.; Ducati, C.; Kasama, T.; Dunin-Borkowski, R. E.; Drucker, J.; Bennett, P.; Robertson, J. *Nat. Mater.* **2008**, *7*, 372.
(27) Kim, B. J.; Tersoff, J.; Kodambaka, S.; Reuter, M. C.; Stach, E. A.; Ross, F. M. *Science* **2008**, *322*, 1070.
(28) Persson, A. I.; Ohlsson, B. J.; Jeppesen, S.; Samuelson, L. *J. Cryst. Growth* **2004**, *272*, 167.
(29) Jeppsson, M.; Dick, K. A.; Wagner, J. B.; Caroff, P.; Deppert, K.; Samuelson, L.; Wernersson, L. E. *J. Cryst. Growth* **2008**, *310*, 4115.
(30) Paek, J. H.; Nishiwaki, T.; Yamaguchi, M.; Sawaki, N. *Phys. Status Solidi C* **2004**, *4*, 1961.
(31) Tomioka, K.; Motohisa, J.; Hara, S.; Fukui, T. *Nano Lett.* **2008**, *8*, 3475.
(32) Sato, T.; Motohisa, J.; Noborisaka, J.; Hara, S.; Fukui, T. *J. Cryst. Growth* **2008**, *310*, 2359.
(33) Jensen, L. E.; Bjork, M. T.; Jeppesen, S.; Persson, A. I.; Ohlsson, B. J.; Samuelson, L. *Nano Lett.* **2004**, *4*, 1961.
(34) Verheijen, M. A.; Immink, G.; de Smet, T.; Borgström, M. T.; Bakkers, E. P. A. M. *J. Am. Chem. Soc.* **2006**, *128*, 1353.
(35) Borgstrom, M. T.; Immink, G.; Ketelaars, B.; Algra, R.; Bakkers, E. P. A. M. *Nat. Nanotechnol.* **2007**, *2*, 541.
(36) Dick, K. A.; Deppert, K.; Karlsson, L. S.; Wallenberg, L. R.; Samuelson, L.; Seifert, W. *Adv. Funct. Mater.* **2005**, *15*, 1603.

(37) Mattila, M.; Hakkarainen, T; Lipsanen, H.; Jiang, H.; Kauppinen, E. I. *Appl. Phys. Lett.* **2006**, *89*, 063119.

(38) Jabeen, F.; Grillo, V.; Rubini, S.; Martelli, F. *Nanotechnology* **2008**, *19*, 275711.

(39) Novotny, C. J.; Yu, P. K. L. *Appl. Phys. Lett.* **2005**, *87*, 203111.

(40) Stach, E. A.; Pauzauskie, P. J.; Kuykendall, T.; Goldberger, J.; He, R.; Yang, P. *Nano Lett.* **2003**, *3*, 867.

(41) Woo, R. L.; Xiao, R.; Kobayashi, Y.; Gao, L.; Goel, N.; Hudait, M. K.; Mallouk, T. E.; Hicks, R. F. *Nano Lett.* **2008**, *8*, 4664.

(42) Lide, D. R. *CRC Handbook of Chemistry and Physics*, 84th ed.; CRC Press: Boca Raton, FL, 2003.

(43) Stringfellow, G. B. *Organometallic Vapor-Phase Epitaxy: Theory and Practice*; Academic Press: San Diego, CA, 1989.

(44) Woo, R. L.; Das, U.; Cheng, S. F.; Chen, G.; Raghavachari, K.; Hicks, R. F. *Surf. Sci.* **2006**, *600*, 4888.

(45) Liehr, M.; Greenlief, C. M.; Kasi, S. R.; Offenberg, M. *Appl. Phys. Lett.* **1990**, *56*, 629.

(46) Kipp, L.; Bringans, R. D.; Biegelsen, D. K.; Swartz, L.-E.; Hicks, R. F. *Phys. Rev. B* **1994**, *50*, 5448.

(47) Givargizov, E. I. *J. Cryst. Growth* **1975**, *31*, 20.

(48) Dubrovskii, V. G.; Sibirev, N. V.; Cirlin, G. E.; Harmand, J. C.; Ustinov, V. M. *Phys. Rev. E* **2006**, *73*, 021603.

(49) Sun, Y.; Law, D. C.; Visbeck, S. B.; Hicks, R. F. *Surf. Sci.* **2002**, *513*, 256.